I am greatly indebted to Professor Peder Kierkegaard for his encouraging interest in this work and for the facilities placed at my disposal. Thanks are also due to Dr Don Koenig for valuable comments on the manuscripts and for his correction of the English of this paper.

References

COCHRAN, W. (1952). *Acta Cryst.* **5**, 65.
COCHRAN, W. (1955). *Acta Cryst.* **8**, 473.
GERMAIN, G., MAIN, P. & WOOLFSON, M. M. (1970). *Acta Cryst.* B**26**, 274.
GLEHN, M. VON, NORRESTAM, R., KIERKEGAARD, P., MARON, L. & ERNSTER, L. (1972). *F.E.B.S. letters*, **20**, 267.
HAUPTMAN, H. (1964). *Acta Cryst.* **17**, 1421.
HAUPTMAN, H. (1970). *Acta Cryst.* B**26**, 531.
HAUPTMAN, H., FISHER, J. & HANCOCK, H. (1969). *Acta Cryst.* B**25**, 811.
HAUPTMAN, H. & KARLE, J. (1953). *Acta Cryst.* **6**, 136.
HAUPTMAN, H. & KARLE, J. (1956). *Acta Cryst.* **9**, 45.
HUGHES, E. W. (1953). *Acta Cryst.* **6**, 871.
KARLE, I. L., KARLE, J. & ESTLIN, J. A. (1967). *Acta Cryst.* **23**, 494.
KARLE, J. & HAUPTMAN, H. (1956). *Acta Cryst.* **9**, 635.
KARLE, J. & HAUPTMAN, H. (1961). *Acta Cryst.* **14**, 217.
KARLE, J. & KARLE, I. L. (1966). *Acta Cryst.* **21**, 849.
KIHLBORG, L., NORRESTAM, R. & OLIVECRONA, B. (1971). *Acta Cryst.* B**27**, 2066.
NORRESTAM, R. (1971). *Acta Chem. Scand.* **25**, 1040.
NORRESTAM, R. (1972). *Acta Cryst.* B**28**, 1713.
NORRESTAM, R. & VON GLEHN, M. (1972). To be published.
SAYRE, D. M. (1952). *Acta Cryst.* **5**, 60.

Acta Cryst. (1972). A**28**, 308

The One-Dimensional Anti-Phase Domain Structures. III. An Alternative Interpretation of the Structure with a Non-Integral Value of the Half Period, $\tilde{M}$

BY TERUAKI MINAGAWA*

Department of Physics, Faculty of Science, Osaka City University, 459 Sugimoto-cho, Sumiyoshi-ku, Osaka, Japan

(*Received* 24 *August* 1971 *and in revised form* 17 *November* 1971)

The non-integral value for the half period, $\tilde{M}$($M<\tilde{M}<M+1$, M:integer), as experimentally found in one-dimensional anti-phase domain structures, is explained by a disordered structure consisting of a mixture of two kinds of structure units with thicknesses of M and $M+1$ layers. The diffraction intensity for the disordered structure is calculated by the use of the general diffraction theory for a one-dimensionally disordered crystal given by Kakinoki & Komura [*Acta Cryst.* (1965), **19**, 137]. With this model the non-integral value of the half period, $\tilde{M}$, can be explained as due to the shift between two peaks, one due to a simple APD (anti-phase domain) structure with half period, M, and the other to another simple APD structure with half period, $M+1$. It is not necessary to consider a very large value of the period as was required in Fujiwara's model [Fujiwara, *J. Phys. Soc. Japan* (1957), **12**, 7], which was proposed assuming a disordered structure, deviating from the standard structure defined by a step function.

1. Introduction

In some examples of one-dimensional anti-phase domain structures with an out-of-step vector $\mathbf{u}=(\mathbf{a}+\mathbf{b})/2$, the half period, $\tilde{M}$, has experimentally been found to be non-integral, as shown in Table 1. Fujiwara (1957) explained this by assuming a disordered structure deviating from a standard structure which is defined by the use of a step function. The interpretation of the non-integral structure and the relevant intensity equations were discussed in detail in part II of this series (Kakinoki & Minagawa, 1972). In Fujiwara's interpretation, however, the period P of the standard structure should be subject to the relation

$$P=2\nu\tilde{M} \tag{1}$$

where ν is the minimum positive integer to make $2\nu\tilde{M}$ equal to an integer P [refer to equation (F–4)†]. Therefore, if we put

$$\tilde{M}=M+\Delta M \quad \text{with} \quad 0<\Delta M<1 \tag{2}$$

where M is an integer, then we have to assume a very high value of P, *e.g.*, $P=321$ for $\tilde{M}=3{\cdot}21$ ($M=3$,

* Present address: Department of Physics, Osaka Kyoiku University, Tennoji, Osaka, Japan.

† Equation (F–4) means equation (4) in Fujiwara's (1957) paper.

$\Delta M = 0{\cdot}21$), and $P = 3213$ for $\tilde{M} = 3{\cdot}213$, *etc.* However, such long periods seem to be unrealistic.

In the present paper, we propose an alternative model of a disordered structure which is composed of two kinds of structure units with thicknesses of M and $M+1$ layers, where $M < \tilde{M} < M+1$. By this model, the non-integral half period, $\tilde{M}$, is more reasonably interpreted without assuming a very large value of P, and $\tilde{M}$ is understood to be due to the shift from the peak for the simple APD (anti-phase domain) structure, $(M \mid \overline{M})$,* to that for the simple APD structure, $(M+1 \mid \overline{M+1})$.*

Table 1. *Examples of the alloys with non-integral values for the half period, $\tilde{M}$*

Alloy	$\tilde{M}$	Reference
Ag_3Mg	1·77 ~ 2·0	(*a*), (*b*)
Cu_3Au II	8 ~ 10	(*c*), (*d*), (*e*)
Cu_3Pt	6 ~ 8	(*a*)
$Cu_{3+}Pd$	7 ~ 11	(*a*), (*f*), (*g*)
CuAu II	5 ~ 6	(*h*), (*i*)

(*a*): Schubert, Kiefer, Wilkens & Haufler (1955).
(*b*): Fujiwara, Hirabayashi, Watanabe & Ogawa (1958).
(*c*): Scott (1960).
(*d*): Yakel (1962).
(*e*): Yamaguchi, Watanabe & Ogawa (1962).
(*f*): Watanabe & Ogawa (1956).
(*g*): Hirabayashi & Ogawa (1957).
(*h*): Jehanno & Pério (1962).
(*i*): Toth & Sato (1962).

2. The present model

The present model consists of a disordered structure composed of alternate series of M or $M+1$ positive and negative layers, as illustrated in the continuing table shown as Table 2, where (M) and $(M+1)$ represent the units consisting of successive M and $M+1$ positive layers respectively, and $(\overline{M})$ and $(\overline{M+1})$ are those of successive M and $M+1$ negative layers respectively. Here, the positive and the negative layers mean the layers without and with the out-of-step vector **u** respectively, as shown in Fig. 1. Table 2 implies that the unit (M) [or $(\overline{M})$] is followed by the unit $(\overline{M})$ [or (M)] with a probability, α, and the unit $(M+1)$ [or $(\overline{M+1})$] is followed by the unit $(\overline{M+1})$ [or $(M+1)$] with a probability, β, *etc.* In no case is a unit followed by a unit with the same sign, *i.e.*, for example, the unit (M) is in no case followed by the units (M) or $(M+1)$.

Table 2. *The continuing table*

	(M)	$(M+1)$	$(\overline{M})$	$(\overline{M+1})$
(M)	0	0	α	$1-\alpha$
$(M+1)$	0	0	$1-\beta$	β
$(\overline{M})$	α	$1-\alpha$	0	0
$(\overline{M+1})$	$1-\beta$	β	0	0

If the existence probabilities of the four units (M), $(M+1)$, $(\overline{M})$ and $(\overline{M+1})$, are denoted by f_1, f_2, f_3 and f_4 respectively, we obtain

$$\begin{cases} f_1 = f_3 = \frac{1}{2} w_1 & w_1 = \dfrac{1-\beta}{2-\alpha-\beta} \\ f_2 = f_4 = \frac{1}{2} w_2 & w_2 = \dfrac{1-\alpha}{2-\alpha-\beta} \end{cases} \tag{3}$$

with

$$f_1 + f_2 + f_3 + f_4 = w_1 + w_2 = 1 .$$

Relations (3) follow from equation [12],† *i.e.*

$$\mathbf{HP} = \mathbf{H} \quad \text{and spur } \mathbf{H} = 1 \tag{4}$$

which is a self-consistent relation between the existence and the continuing probabilities. In the present case, **H** and **P** are matrices of order 4, and are expressed as

$$\mathbf{H} = \begin{bmatrix} f_1 & f_2 & f_3 & f_4 \\ f_1 & f_2 & f_3 & f_4 \\ f_1 & f_2 & f_3 & f_4 \\ f_1 & f_2 & f_3 & f_4 \end{bmatrix}$$

and

$$\mathbf{P} = \begin{bmatrix} 0 & 0 & \alpha & 1-\alpha \\ 0 & 0 & 1-\beta & \beta \\ \alpha & 1-\alpha & 0 & 0 \\ 1-\beta & \beta & 0 & 0 \end{bmatrix} . \tag{5}$$

Using equation (3), we can rewrite **H** and **P**, by the use of minor matrices of order 2, as

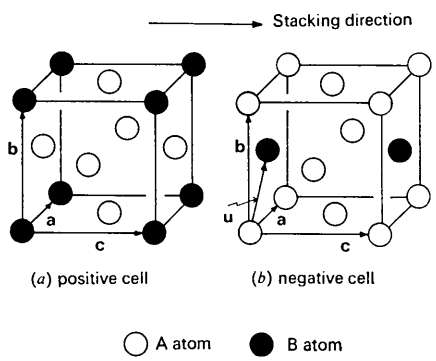

Fig. 1. Two kinds of unit cell in the one-dimensional anti-phase domain structure of A_3B-type with an out-of-step vector $\mathbf{u} = (\mathbf{a}+\mathbf{b})/2$.

* For the classification of the one-dimensional anti-phase domain structures, *i.e.* a complex out-of-step structure, a complex APD structure and a simple APD structure, and the corresponding notations, refer to part I of this series (Kakinoki & Minagawa, 1971).

† Equation numbers in [ ] are those of Kakinoki & Komura (1965).

$$\mathbf{H}=\tfrac{1}{2}\begin{bmatrix}\mathbf{h} & \mathbf{h}\\ \mathbf{h} & \mathbf{h}\end{bmatrix} \text{ with } \mathbf{h}=\begin{bmatrix}w_1 & w_2\\ w_1 & w_2\end{bmatrix},$$
$$\mathbf{P}=\begin{bmatrix}0 & \mathbf{p}\\ \mathbf{p} & 0\end{bmatrix} \text{ with } \mathbf{p}=\begin{bmatrix}\alpha & 1-\alpha\\ 1-\beta & \beta\end{bmatrix}. \tag{6}$$

Thus, equation (4) is equivalent to the relations

$$\mathbf{hp}=\mathbf{h} \text{ and } \operatorname{spur}\mathbf{h}=1\,. \tag{7}$$

Corresponding to this reduction of the order of the matrices from 4 to 2, Table 2 may be rewritten as a 'convenient continuing table', shown as Table 3, where $\{M\}$ represents the unit (M) or $(\bar{M})$ and $\{M+1\}$ represents the unit $(M+1)$ or $(\overline{M+1})$ and two units with the same sign are prohibited from following one another.

Table 3. *The convenient continuing table*

	$\{M\}$	$\{M+1\}$
$\{M\}$	α	$1-\alpha$
$\{M+1\}$	$1-\beta$	β

From Table 3, together with equations (3) and (7), we can derive the following four special cases:

(1) When $\alpha=1$ and $0\le\beta<1$, we have $w_1=1$ and $w_2=0$ and get a simple APD structure, $(M\mid\bar{M})$ with $P=2M$. The corresponding unitary intensities of the superlattice reflexions are given by

$$\begin{cases} I_l=0 & \text{for } l\text{: even}\\ I_l=\dfrac{4}{\sin^2\dfrac{\pi l}{P}} & \text{for } l\text{: odd}\end{cases} \tag{8}$$

[refer to equation (I-16)†]. I_l's are schematically shown in Fig. 2(*a*) for the case of $M=3$, where ζ is the parameter along $\mathbf{c}^*$, $\mathbf{c}^*$ being the vector reciprocal to $\mathbf{c}$, and

$$\zeta=\frac{l}{P}\quad l\text{: } 0,\ \pm1,\ \pm2,\ \pm3,\ \ldots. \tag{9}$$

(2) When $\beta=1$ and $0\le\alpha<1$, we have $w_1=0$ and $w_2=1$ and get another simple APD structure, $(M+1\mid\overline{M+1})$ with $P=2(M+1)$. The corresponding unitary intensities of the superlattice reflexions are schematically shown in Fig. 2(*c*) for the case of $M=3$.

(3) When $\alpha=\beta=1$, we have only $w_1+w_2=1$ from equation (7) and we get a mixture of the two structures $(M\mid\bar{M})$ and $(M+1\mid\overline{M+1})$ with arbitrary weights, w_1 and $w_2=1-w_1$.

(4) When $\alpha=\beta=0$, we have $w_1=w_2=\frac{1}{2}$ and we get a structure $(M\,\overline{M+1})$ or $(M+1\;\bar{M})$ with $P=2M+1$, which is the simplest structure of the complex out-of-step structures.‡ The corresponding unitary intensities of the superlattice reflexions are given by

$$\begin{cases} I_l=\dfrac{1}{\cos^2\dfrac{\pi l}{2P}} & \text{for } l\text{: even}\\ I_l=\dfrac{1}{\sin^2\dfrac{\pi l}{2P}} & \text{for } l\text{: odd}\end{cases} \tag{10}$$

‡ Refer to second footnote in § 1.

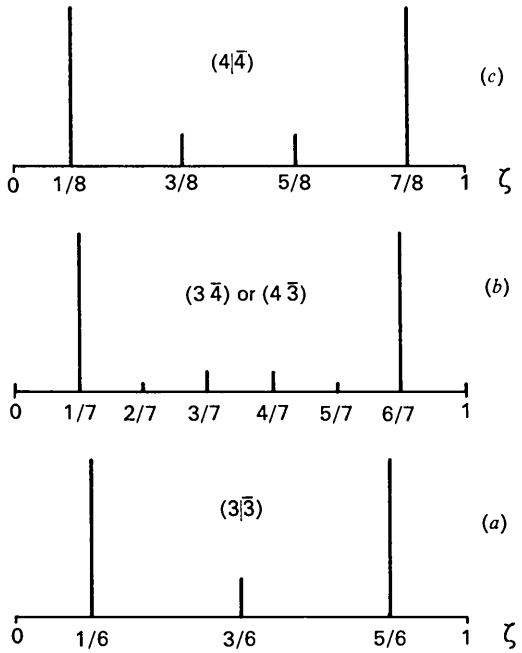

Fig. 2. Unitary intensities of superlattice reflexions for $(3\mid\bar{3})$, $(3\,\bar{4})$ or $(4\,\bar{3})$ and $(4\mid\bar{4})$.

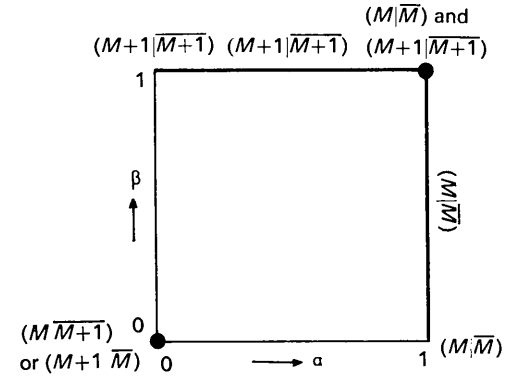

Fig. 3. The locations corresponding to the four special cases in the (α,β)-map.

† The equation numbers in part I of this series (Kakinoki & Minagawa, 1971) are written as (I-1), (I-2), *etc.* The unitary intensity is here expressed excluding the Laue function [refer to I_l in equation (I-6)].

[refer to (I-15)]. I_l's are schematically shown in Fig. 2(*b*) for the case of $M=3$.

These four special cases are shown by the points and lines in the '(α,β)-map' shown in Fig. 3. Case (1) corresponds to the vertical line passing through the point (1,0) on the map, case (2) to the horizontal line passing through the point (0,1), case (3) to the point (1,1) and case (4) to the point (0,0).

It is expected from Fig. 3 together with Fig. 2 that, if we start from the point (1,0) on the (α,β)-map, go to the left along the α axis to the point (0,0), and go up along the β axis to the point (0,1), then, for the disordered structure composed of the units $\{3\}$ ($\{M\}$) and $\{4\}$ ($\{M+1\}$), the strongest peak in the diffraction pattern turns out to shift gradually from $\zeta=\frac{1}{6}$ to $\zeta=\frac{1}{8}$ passing over $\zeta=\frac{1}{7}$ in Fig. 2, without any appreciable loss in its sharpness. Thus, the non-integral value for the half period, $\tilde{M}$, in the one-dimensional anti-phase domain structure can be naturally explained by the present model without introducing a very large value of the period P.

3. The intensity equation

The diffraction intensity for the present model can be straightforwardly calculated by the use of the general theory of Kakinoki & Komura (1965) for one-dimensionally disordered crystals. The present model corresponds to the case of different thicknesses in their theory, and the intensity equation is given by their equation [1], *i.e.*

$$I_0(\varphi)=NB_0+\sum_{m=1}^{N-1}(N-m)B_m+\text{conj.} \qquad (11)$$

with

$$B_m=\text{spur } \mathbf{VFQ}^m,\ \mathbf{Q}=\mathbf{\Phi P} \text{ and } \varphi=2\pi\zeta \qquad (12)$$

where N is the total number of units $\{M\}$ and $\{M+1\}$, and conj. means the complex conjugate of the foregoing term. The meaning of the matrices $\mathbf{V}$, $\mathbf{F}$, $\mathbf{Q}$, $\mathbf{\Phi}$ and $\mathbf{P}$ will be explained below for the present model.

If the structure factor of the positive cell [Fig. 1(*a*)] is denoted by V, the structure factor of the negative cell [Fig. 1(*b*)] is given by εV, where ε is the phase factor corresponding to the out-of-step vector, $\mathbf{u}=(\mathbf{a}+\mathbf{b})/2$, and

$$\varepsilon=(-1)^{h+k}. \qquad (13)$$

Therefore, the structure factors corresponding to the four units (M), $(M+1)$, $(\bar{M})$ and $(M+1)$ are given by

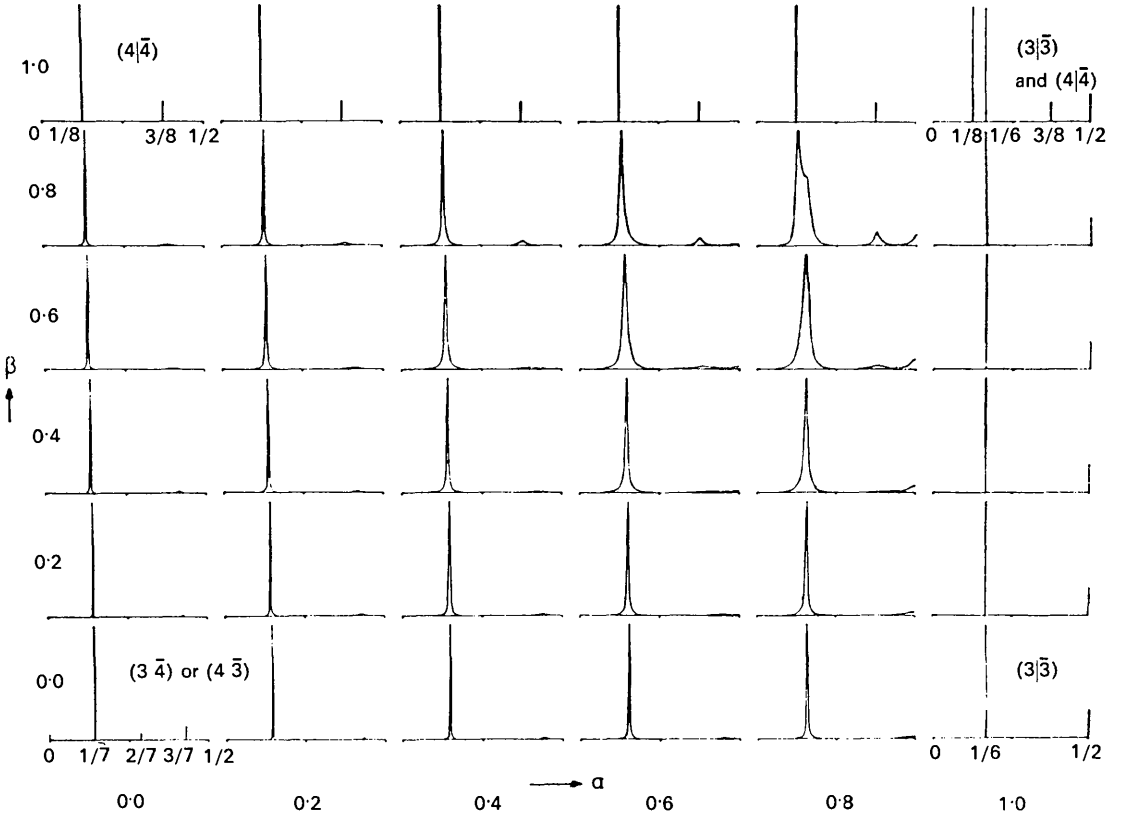

Fig. 4. The curves of $D(\zeta)$ for $M=3$ calculated at intervals, 0·2, of α and β in the half region corresponding to $0\leq\zeta\leq\frac{1}{2}$.

$$\begin{cases} V_1 = V\sum_{n=0}^{M-1} e^{in\varphi} = V\dfrac{\sin M\dfrac{\varphi}{2}}{\sin\dfrac{\varphi}{2}} e^{-i\varphi/2}\, e^{iM\varphi/2} \equiv Vv_1 \\ V_2 = V\sum_{n=0}^{M} e^{in\varphi} = V\dfrac{\sin (M+1)\dfrac{\varphi}{2}}{\sin\dfrac{\varphi}{2}} e^{iM\varphi/2} \equiv Vv_2 \\ V_3 = \varepsilon V_1 \\ V_4 = \varepsilon V_2 \end{cases} \quad (14)$$

respectively, and the matrices **V**, **F**, **Φ** and **Q** in equation (12) are expressed by the use of equation [4] and equations (3), (6) and (14), as follows:

$$\mathbf{V} = VV^* \begin{bmatrix} \mathbf{v} & \varepsilon\mathbf{v} \\ \varepsilon\mathbf{v} & \mathbf{v} \end{bmatrix} \text{ with } \mathbf{v} = \begin{bmatrix} v_1^* v_1 & v_1^* v_2 \\ v_2^* v_1 & v_2^* v_2 \end{bmatrix} = \begin{bmatrix} G_1^2 & G_1 G_2 e^{i\varphi/2} \\ G_1 G_2 e^{-i\varphi/2} & G_2^2 \end{bmatrix}$$

where

$$G_1 = \frac{\sin M\dfrac{\varphi}{2}}{\sin\dfrac{\varphi}{2}} \text{ and } G_2 = \frac{\sin (M+1)\dfrac{\varphi}{2}}{\sin\dfrac{\varphi}{2}},$$

$$\mathbf{F} = \tfrac{1}{2}\begin{bmatrix} \mathbf{w} & 0 \\ 0 & \mathbf{w} \end{bmatrix} \text{ with } \mathbf{w} = \begin{bmatrix} w_1 & 0 \\ 0 & w_2 \end{bmatrix}, \quad (15)$$

$$\mathbf{\Phi} = \phi\begin{bmatrix} \boldsymbol{\phi} & 0 \\ 0 & \boldsymbol{\phi} \end{bmatrix} \text{ with } \boldsymbol{\phi} = \begin{bmatrix} 1 & 0 \\ 0 & e^{-i\omega} \end{bmatrix} \text{ and } \phi = e^{-iM\varphi},$$

$$\mathbf{Q} = \mathbf{\Phi P} = \phi\begin{bmatrix} 0 & \mathbf{q} \\ \mathbf{q} & 0 \end{bmatrix} \text{ with } \mathbf{q} = \boldsymbol{\phi}\mathbf{p} = \begin{bmatrix} \alpha & 1-\alpha \\ (1-\beta)e^{-i\varphi} & \beta e^{-i\varphi} \end{bmatrix}.$$

Thus, B_m given by equation (12) is calculated as

$$B_m = \text{spur } \mathbf{VFQ}^m = VV^*(\varepsilon\phi)^m \text{ spur } \mathbf{vwq}^m \equiv VV^* b_m. \quad (16)$$

As a result, from equation (11) the unitary intensity $I(\varphi)$ is given as

$$I(\varphi) = \frac{I_0(\varphi)}{VV^*} = Nb_0 + \sum_{m=1}^{N-1}(N-m)b_m + \text{conj.} \equiv ND(\varphi) + H(\varphi) \quad (17)$$

with

$$b_m = (\varepsilon\phi)^m \text{ spur } \mathbf{vwq}^m$$
$$(= \exp\{-im(M\varphi - \pi)\} \text{ spur } \mathbf{vwq}^m \text{ for } h+k\text{: odd}). \quad (18)$$

Here, $D(\varphi)$ is the diffuse term and $H(\varphi)$ the higher term. By calculation using the method of Kakinoki & Komura (1965) we obtain the result that (see Appendix I),

$$D(\varphi) = \frac{2(1-\alpha)(1-\beta)(\alpha+\beta)}{2-\alpha-\beta} \Big/ \left(\begin{array}{l} 1-\alpha-\beta+\alpha^2+\beta^2+\alpha\beta+\alpha\beta\cos\varphi+\{\alpha-\beta+\beta(\alpha+\beta)\}\cos M\varphi \\ +\{\beta-\alpha+\alpha(\alpha+\beta)\}\cos(M+1)\varphi-(1-\alpha-\beta)\cos(2M+1)\varphi \end{array}\right) \quad (19)$$

for $h+k$: odd, *i.e.* $\varepsilon=-1$, and that $H(\varphi)$ is usually negligible. However, the four special cases shown in Fig. 3 are exceptions. In these cases $D(\varphi)=0$ and $H(\varphi)$ is given by equation (8) or equation (10) multiplied by the corresponding Laue function with $N_0=N/2$ (see Appendix II).

4. Results

The intensity distribution, $D(\varphi)$, with $\varphi=2\pi\zeta$ [equation (12)], is found to be symmetrical with respect to the points $\varphi=0$ and 180°, or $\zeta=0$ and $\frac{1}{2}$. Here, it is more convenient to use ζ than φ since the main peak is observed corresponding to $\zeta=1/(2\tilde{M})$. The diffuse term, $D(\varphi)$ or $D(\zeta)$, given by equation (19), is computed for M from 1 to 15 and for α and β from 0·0 to 1·0, at intervals of 0·1. Fig. 4 shows the curves of $D(\zeta)$ for $M=3$

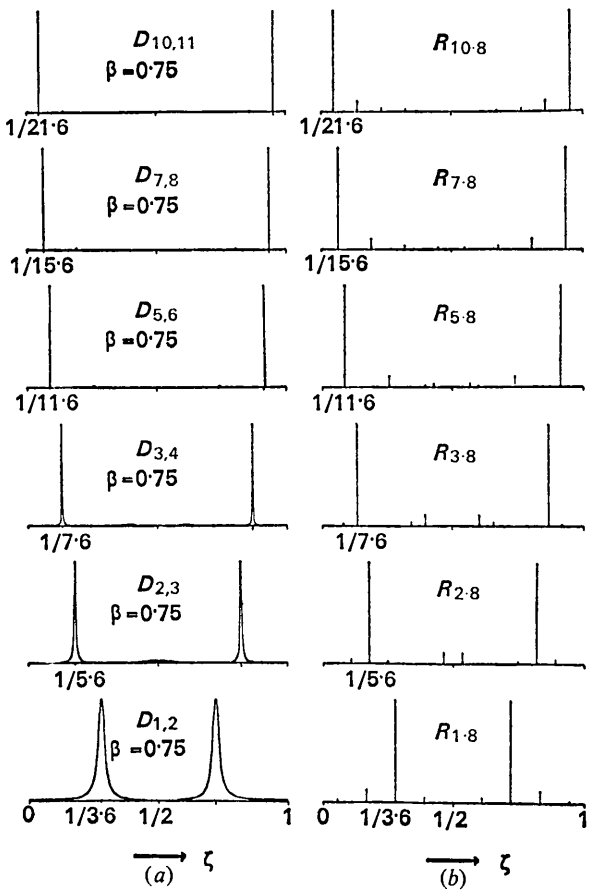

Fig. 5. Unitary intensities in the case of $h+k$: odd calculated from the present model denoted as $D_{M,M+1}$ (*a*) and from the 'regular arrangement with uniform mixing' denoted as $R_{M+\Delta M}$ by Fujiwara (*b*). They are calculated with $\tilde{M}=M+0·8$ for $M=1$, 2, 3, 5, 7 and 10 and then the strongest peak appears at $\zeta=1/(2\tilde{M})$ in each curve.

calculated at intervals of 0·2, in α and β in the half region corresponding to $0 \le \zeta \le \frac{1}{2}$. In order to show the detailed features of the intensity distributions, the intensity scale in Fig. 4 has been chosen so that the strongest intensity has the value unity, while Table 4 gives the calculated values of the strongest intensities in the individual curves. Thus, the absolute intensity of each curve in Fig. 4 is obtained by multiplying by the corresponding value in Table 4. Strictly speaking, the intensity thus calculated should be further multiplied by the factor $4/(3+w_2)$* in order to be appropriate to the correct irradiated volume of the sample.

Table 4. *The calculated values of the strongest intensities in the individual curves in Fig.* 4

β \ α	0·0	0·2	0·4	0·6	0·8	1·0
1·0	L.P.	L.P.	L.P.	L.P.	L.P.	L.P.
0·8	197	115	67	38	19	L.P.
0·6	182	103	60	34	22	L.P.
0·4	248	131	77	47	36	L.P.
0·2	494	204	112	71	58	L.P.
0·0	L.P.	437	188	113	92	L.P.

L.P.: Laue peak.

The results of the computed $D(\zeta)$ are summarized as follows:

(1) It is found from Fig. 4 that the intensity distribution of the strongest peak is relatively sharp when $\beta=0$ (α axis) or $\alpha=0$ (β axis), in accordance with our expectation mentioned in §2. In other words, as we start from the point (1,0) in Fig. 4, go to the left along the α axis to the point (0,0) and go up along the β axis to the point (0,1), the strongest peak gradually shifts from $\zeta_1=\frac{1}{6}$, corresponding to the simple APD structure, $(3 \mid \bar{3})$, to $\zeta_1=\frac{1}{8}$, corresponding to another simple APD structure, $(4 \mid \bar{4})$, passing over $\zeta_1=\frac{1}{7}$, corresponding to the structure, $(3\bar{4})$ or $(4\bar{3})$. Thus, the non-integral value for the half period, $\tilde{M}$, is given as $\tilde{M}=1/(2\zeta_1)$ by the present model assuming the disordered structure to be composed of the units $\{M\}$ and $\{M+1\}$.

(2) The intensity ratio of the second strongest peak at ζ_3† to the strongest one at $\zeta_1=1/(2\tilde{M})$ decreases from about 0·025 to about 0·010‡ as M increases from 2 to 15. These values are so small that only a set of satellites corresponding to $\pm\zeta_1$ would be observable in practice.

(3) The half width of the strongest peak decreases with increasing M as shown in Fig. 5(*a*), where $D(\zeta)$ with $\alpha=0$ and $\beta=0{\cdot}75$ are plotted for $M=1$, 2, 3, 5, 7 and 10, denoted as $D_{M,M+1}$. It can be seen that each plot has the strongest peak at $\zeta_1=1/(2\tilde{M})$ with $\tilde{M}\simeq M+0{\cdot}8$ and that the ratio of the half width of the peak to one period corresponding to the distance between $\zeta=0$ and $\zeta=1$ is less than $\frac{1}{3\cdot5}$ even for $M=1$, so that the corresponding spot is not diffuse but remains relatively sharp.

5. True mean domain size, $\langle M \rangle$

In papers referred to so far, the *mean domain size* has been defined as $\tilde{M}=1/(2\zeta_1)$, where ζ_1 is the ζ value of the strongest peak. This conventional terminology comes by analogy with the fact that, in the case of the simple APD structure, an integral half period, M, is correctly given by $1/(2\zeta_1)$ or by $3/(2\zeta_3)$, where ζ_3 is the ζ-value of the second strongest peak with $l=3$ in equation (8). On the other hand, in the present model, the *true mean domain size*, $\langle M \rangle$, may be defined as

$$\langle M \rangle = w_1 M + w_2(M+1) = M + w_2 = M + \frac{1-\alpha}{2-\alpha-\beta}. \tag{20}$$

* Refer to equation (20).

† The suffix, 3, in ζ_3 comes from the fact that the second strongest peak appears at $l=3$ in the case of the simple APD structure as can be seen from equation (8).

‡ In the simple APD structure, the intensity ratio is expressed as $\sin^2(\pi/2M)/\sin^2(3\pi/2M)$ by equation (8); for example, the intensity ratios are about $\frac{1}{4}$, $\frac{1}{6}$ and $\frac{1}{7}$ in the cases of $(3 \mid \bar{3})$, $(4 \mid \bar{4})$ and $(5 \mid \bar{5})$ respectively.

Table 5. *The structures corresponding to the model of regular arrangements with uniform mixing in the cases of* $\Delta M=0{\cdot}1, 0{\cdot}2, \ldots, 0{\cdot}9$ *and the corresponding period,* P, *given by equation* (1)

$\tilde{M}$	P	Structure*	Symbol
M	$2M$	$(M \mid \bar{M})$	R_M
$M+0{\cdot}1$	$10M+1$	$(M+1\ \bar{M}\ M\ \bar{M}\ M\ \bar{M}\ M\ \bar{M}\ M\ \bar{M})$	$R_{M+0\cdot1}$
$M+0{\cdot}2$	$10M+2$	$((M+1\ \bar{M}\ M\ \bar{M}\ M) \mid (\overline{M+1}\ M\ \bar{M}\ M\ \bar{M}))$	$R_{M+0\cdot2}$
$M+0{\cdot}3$	$10M+3$	$(M+1\ \bar{M}\ M\ \overline{M+1}\ M\ \bar{M}\ M+1\ \overline{M}\ M\ \bar{M})$	$R_{M+0\cdot3}$
$M+0{\cdot}4$	$10M+4$	$((M+1\ \bar{M}\ M+1\ \bar{M}\ M) \mid (\overline{M+1}\ M\ \overline{M+1}\ M\ \bar{M}))$	$R_{M+0\cdot4}$
$M+0{\cdot}5$	$2M+1$	$(M+1\ \bar{M})$	$R_{M+0\cdot5}$
$M+0{\cdot}6$	$10M+6$	$((M+1\ \overline{M+1}\ M\ \overline{M+1}\ M) \mid (\overline{M+1}\ M+1\ \bar{M}\ M+1\ \bar{M}))$	$R_{M+0\cdot6}$
$M+0{\cdot}7$	$10M+7$	$(M+1\ \overline{M+1}\ M+1\ \bar{M}\ M+1\ \overline{M+1}\ M\ \overline{M+1}\ M+1\ \bar{M})$	$R_{M+0\cdot7}$
$M+0{\cdot}8$	$10M+8$	$((M+1\ \overline{M+1}\ M+1\ \overline{M+1}\ M) \mid (\overline{M+1}\ M+1\ \overline{M+1}\ M+1\ \bar{M}))$	$R_{M+0\cdot8}$
$M+0{\cdot}9$	$10M+9$	$(M+1\ \overline{M+1}\ M+1\ \overline{M+1}\ M+1\ \overline{M+1}\ M+1\ \overline{M+1}\ M+1\ \bar{M})$	$R_{M+0\cdot9}$
$M+1$	$2(M+1)$	$(M+1 \mid \overline{M+1})$	R_{M+1}

* For the notation of the structures, refer to part I of this series (Kakinoki & Minagawa, 1971).

In order to distinguish $\langle M\rangle$ from $\tilde{M}$, $\tilde{M}$ is called the *apparent mean domain size*. Since $1/(2\zeta)_1$ is not always equal to $3/(2\zeta_3)$ for the structure with a non-integral period, we may have two kinds of $\tilde{M}$, one given by half $\tilde{M}_1=1/(2\zeta_1)$ and the other by $\tilde{M}_3=3/(2\zeta_3)$. These three kinds of mean domain sizes, *i.e.* $\langle M\rangle$, $\tilde{M}_1$ and $\tilde{M}_3$, do not always coincide, as can be seen in Fig. 6 where the loci for $\langle M\rangle=\tilde{M}_1=\tilde{M}_3=M+\Delta M$ are shown by dotted, solid* and broken lines respectively, for $M=1$ (*a*), 3 (*b*) and 7 (*c*) at intervals of $\Delta M=0{\cdot}1$. The loci for constant ζ_1 (*i.e.* $\tilde{M}_1$) and constant ζ_3 (*i.e.* $\tilde{M}_3$) are obtained by differentiating $D(\varphi)$ with respect to φ. It is clear from Fig. 6 that $\langle M\rangle$, $\tilde{M}_1$ and $\tilde{M}_3$ do not coincide with one another. Correctly speaking, $\langle M\rangle$ should be obtained by substituting the values of α and β corresponding to the cross point of the loci of observed ζ_1 and ζ_3† into equation (20). Practically speaking, however, because the second strongest peak at ζ_3 is usually too weak to be detected and the strongest peak at ζ_1 is relatively sharp when $\beta=0$ (α axis) or $\alpha=0$ (β axis) as mentioned in §4 (1), the cross points seem to be distributed near the α and β axes where $\langle M\rangle$, $\tilde{M}_1$ and $\tilde{M}_3$ are nearly equal to one another. The differences among them become smaller as M increases, as shown in Fig. 6(*a*), (*b*) and (*c*). In these cases, the apparent mean domain size, $\tilde{M}$, is practically the same as the true mean domain size, $\langle M\rangle$.

6. Discussion

An interpretation of the non-integral value for the half period, $\tilde{M}$, was first given by Fujiwara (1957) using a model of the *regular arrangements with uniform mixing* which is defined by a step function. He refined the model by introducing some disordering, and proposed a model of the *statistical assembly of irregular arrangements*. The intensity expressions for these two models were recently discussed in detail in part II of this series (Kakinoki & Minagawa, 1972).

Table 5 shows some examples of the *regular arrangements with uniform mixing* which, in part II, we called the *standard structures*. These structures with various values of $\tilde{M}=M+\Delta M$ are denoted by $R_{M+\Delta M}$, and some examples of the intensity distributions for $R_{M+0{\cdot}8}$ are shown in Fig. 5(*b*) where $\Delta M=0{\cdot}8$ nearly corresponds to $\alpha=0$ and $\beta=0{\cdot}75$ which are assumed for Fig. 5(*a*). The intensity ratios of the second strongest to the strongest peak in these examples are listed in Table 6.‡ Since these ratios are greater than $\frac{1}{9}$, the second strongest peaks should be strong enough to be observed as are both the second and third strongest peaks from the simple APD structure. In practice, however, the second strongest peak is hardly detectable for non-integral structures. It was for this reason that Fujiwara introduced the model of *statistical assembly of irregular arrangements* which, in part II, we called

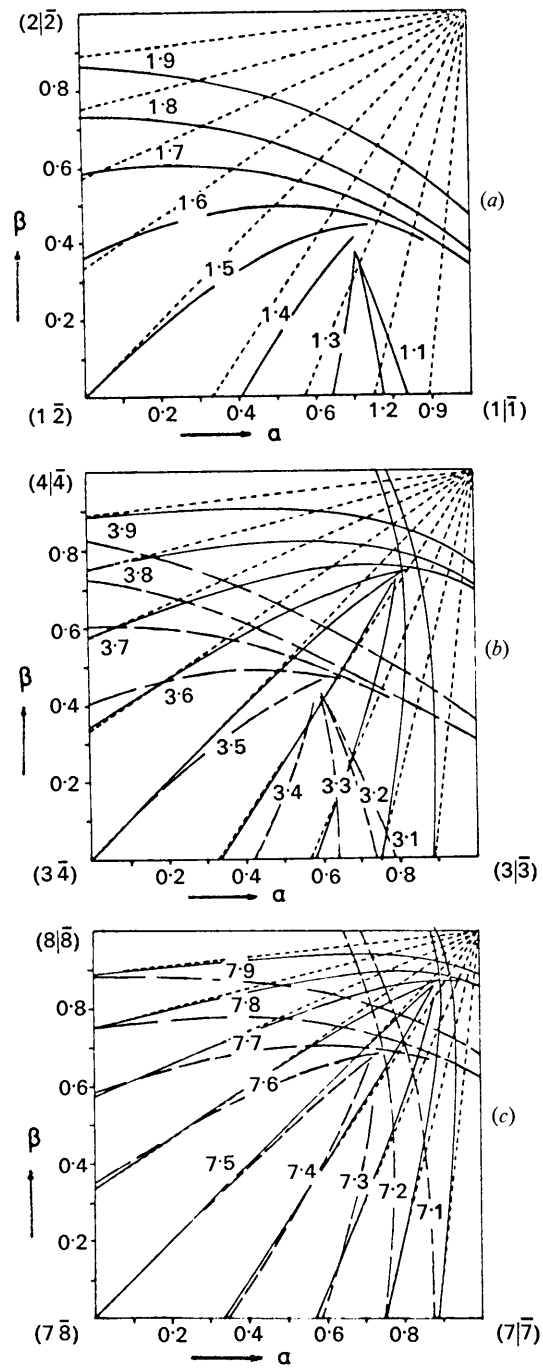

Fig. 6. Loci for the constant values of $\langle M\rangle=M+w_2$ at intervals of 0·1 (dotted straight lines), of $\tilde{M}_1=1/(2\zeta_1)$ at intervals of 0·1 (solid curves) and of $\tilde{M}_3=3/(2\zeta_3)$ at intervals of 0·1 (broken curves). (*a*), (*b*) and (*c*) show the cases of $M=1$, 3 and 7 respectively.

* Some of them disappear at some points. This is because $D(\zeta)$ shows not a maximum but a minimum at ζ_1 after the point.

† When $M=1$ there is no peak at ζ_3.

‡ Refer to equation (II-33). The equation numbers in part II of this series (Kakinoki & Minagawa, 1972) are written as (II-1), (II-2), *etc.*

briefly the *statistical assembly*. According to an intensity equation obtained for this model [refer to (II-46)], the value of the ratio may reduce to any small value including 0, according as a standard deviation, σ, of the distribution function* increases, as shown in Table 7.

Table 6. *The intensity ratios of the second strongest peak to the strongest one in the examples shown in Fig.* 5(*b*)

Structure	Ratio
$R_{10\cdot8}$	0·111
$R_{7\cdot8}$	0·112
$R_{5\cdot8}$	0·112
$R_{3\cdot8}$	0·113
$R_{2\cdot8}$	0·115
$R_{1\cdot8}$	0·121

Table 7. *The intensity ratio of the second strongest peak to the strongest one in the model of statistical assembly of irregular arrangements with* $\tilde{M}=1\cdot8$ *and* $P=18$

Refer to equation (II-46). The ratio decreases with increasing σ, a standard deviation [refer to equation (II-36)].

σ	Ratios
0	0·093
0·05	0·093
0·10	0·086
0·16	0·060
0·20	0·042
0·25	0·024
0·32	0·009
0·40	0·002
0·50	0·00000

As mentioned in the introduction, Fujiwara's model should take account of the very large value of the period P necessitated by equation (1). On the other hand, according to the model introduced in the present paper, the non-integral value for the half period, $\tilde{M}$, is due to the peak shift caused by the disordering between $\{M\}$ and $\{M+1\}$ and it is not necessary to take account of a very large value of P. By the present model, in addition, the intensity of the second strongest peak may become less than 2·5% of that of the strongest one if the half width of the strongest one is sufficiently narrow. Thus, the present model may be an alternative to that of Fujiwara for explaining the non-integral value of the half period.

The appearance of a set of satellites can often be explained qualitatively by assuming a sinusoidal modulation of the lattice as was the case for the superstructure of $NaNO_2$ (Yamada, Shibuya & Hoshino, 1963). However, if the experimental accuracy is not adequate to satisfactorily determine the intensity of the second strongest peak, either of the disordered models given by Fujiwara and by the present author may be taken as a possible model to explain those satellites.

* Refer to equation (II-36).

The present model can easily be generalized by considering many kinds of units such as

$$\ldots, \{M-3\}, \{M-2\}, \{M-1\}, \{M\}, \{M+1\}, \{M+2\}, \{M+3\}, \ldots$$

with appropriate weights, and the weighted mean of them is given by $\tilde{M}$. By this generalization, the ratio of the second strongest intensity to the strongest one may further be reduced.

Fujiwara, Hirabayashi, Watanabe & Ogawa (1958) observed the second strongest peak of very faint intensity in the case of $\tilde{M}=1\cdot77$ (Ag_3Mg). The present model does not seem to be appropriate to this case because it predicts no maximum other than the main peak, as shown by $D_{1,2}$ in Fig. 5(*a*). On the other hand, in cases when $\tilde{M}$ is larger than 2, the situation is quite different because the present model gives a weak, diffuse maximum at the position of the second strongest peak, as shown by $D_{M,M+1}$ other than $D_{1,2}$ in Fig. 5(*a*).

In connexion with the calculation in the present paper, Kakinoki (1971) made the following two comments, which are worth quoting.

(1) If $h+k$ is even, as ε given by equation (13) becomes unity, there is no distinction between the positive and the negative layers, and we should have only the fundamental reflexion, unaccompanied by any superlattice reflexion. In this case, the intensity equation (17) should give the weighted mean of the Laue functions corresponding to the layer numbers from NM to $N(M+1)$ with appropriate weights w_s, *i.e.*

$$\sum_{s=0}^{N} w_s \frac{\sin^2 \pi(NM+s)\zeta}{\sin^2 \pi\zeta} .$$

(2) Another method of calculating the intensity equation for the present model is given by the method similar to that given by Kakinoki & Komura (1965). In this method, the intensity equation is the same as equation (19) with a slight modification in the constant factor for the superlattice reflexions, and it gives a single Laue function (not the weighted mean of the Laue functions) for the fundamental one.

APPENDIX I
Derivation of equation (19)

A method for deriving the intensity equation of the type

$$I_0(\varphi)=NB_0+\sum_{m=1}^{N-1}(N-m)B_m+\text{conj.} \qquad \text{(A1)}$$

$$B_m=\text{spur } \mathbf{VFQ}^m$$

which was given as equation [1] for the case of different thicknesses, was given by Kakinoki & Komura (1965). Their results are summarized as follows:

Step 1: Expand the characteristic equation, equation [33], as

$$\det(y\mathbf{l}-\mathbf{Q})=\sum_{n=0}^{R} a_n y^{R-n} \tag{A2}$$

where R is the order of matrices $\mathbf{V}$, $\mathbf{F}$ and $\mathbf{Q}$ and $a_0=1$.

Step 2: Calculate B_m for m from 0 to $R-1$.

Step 3: Substitute a_n's and B_m's obtained above into equation [40] *i.e.*

$$D(\varphi)=\begin{matrix} D_0+\sum_{p=1}^{R-1} D_p+\text{conj.} \\ C_0+\sum_{p=1}^{R} C_p+\text{conj.} \end{matrix} \tag{A3}$$

where

$$C_p=\sum_{n=0}^{R-p} a_n a_{n+p}^{*} . \tag{A4}$$

$$D_p=\sum_{n=0}^{R-1-p} a_n E_{n+p} \text{ with } E_q=\sum_{m=0}^{R} a_m^{*} B_{m-q} \tag{A5}$$

which were given by equations [41*a*] and [41*c*] respectively.

In the present case, the quantities in these equations become as follows:

$$R=2,\ B_m\to b_m,\ \mathbf{V}\to\mathbf{v},\ \mathbf{F}\to\mathbf{w},\ \mathbf{Q}\to\varepsilon\phi\mathbf{q} \tag{A6}$$

and

$$\begin{cases} D_1=b_1^{*}+a_1^{*}b_0+a_2^{*}b_1 , \\ D_0=a_1 b_1^{*}+a_1^{*}b_1+(1+a_1a_1^{*}-a_2a_2^{*})b_0 \end{cases} \tag{A7}$$

which were given by equation [42*b*] with equation [42*a*]. Hence, the above three steps are carried out by the use of equations (3), (6), (14), (15) and (18) as below:

Step 1:

$$\mathbf{Q}\to\varepsilon\phi\mathbf{q}=\varepsilon\phi\begin{bmatrix}\alpha & 1-\alpha\\ (1-\beta)e^{-i\varphi} & \beta e^{-i\varphi}\end{bmatrix}.$$

Therefore

$$\begin{aligned}\det(y\mathbf{l}-\mathbf{Q})\to&\begin{vmatrix} y-\alpha\varepsilon\phi & -(1-\alpha)\varepsilon\phi \\ -\varepsilon\phi(1-\beta)e^{-i\varphi} & y-\varepsilon\phi\beta e^{-i\varphi}\end{vmatrix}\\ &=y^2-\varepsilon\phi(\alpha+\beta e^{-i\varphi})y-(1-\alpha-\beta)\phi^2e^{-i\varphi}.\end{aligned}$$

Thus, we have

$$a_1=-\varepsilon\phi(\alpha+\beta e^{-i\varphi}),\quad a_2=-(1-\alpha-\beta)\phi^2e^{-i\varphi}. \tag{A8}$$

Step 2:

$$\mathbf{V}\to\mathbf{v}=\begin{bmatrix}v_1^{*}v_1 & v_1^{*}v_2\\ v_2^{*}v_1 & v_2^{*}v_2\end{bmatrix}=\begin{bmatrix}G_1^2 & G_1G_2e^{i\varphi/2}\\ G_1G_2e^{i\varphi/2} & G_2^2\end{bmatrix}$$

with

$$G_1=\frac{\sin M\frac{\varphi}{2}}{\sin\frac{\varphi}{2}} \text{ and } G_2=\frac{\sin(M+1)\frac{\varphi}{2}}{\sin\frac{\varphi}{2}} \tag{A9}$$

and hence,

$$\begin{aligned}B_m\to b_m=(\varepsilon\phi)^m\ &\text{spur}\ \mathbf{vwq}^m\\ =\frac{(\varepsilon\phi)^m}{2-\alpha-\beta}\ &\text{spur}\begin{bmatrix}(1-\beta)G_1^2 & (1-\alpha)G_1G_2e^{i\varphi/2}\\ (1-\beta)G_1G_2e^{-i\varphi/2} & (1-\alpha)G_2^2\end{bmatrix}\\ &\times\begin{bmatrix}\alpha & 1-\alpha\\ (1-\beta)e^{-i\varphi} & \beta e^{-i\varphi}\end{bmatrix}^m,\end{aligned}$$

from which we have

$$\begin{cases} b_0=\dfrac{1}{2-\alpha-\beta}\{(1-\beta)G_1^2+(1-\alpha)G_2^2\}, \\ b_1=\dfrac{\varepsilon\phi}{2-\alpha-\beta}\{\alpha(1-\beta)G_1^2+\beta(1-\alpha)G_2^2e^{-i\varphi} \\ \quad +2(1-\alpha)(1-\beta)G_1G_2e^{-i\varphi/2}\}. \end{cases} \tag{A10}$$

Step 3:

$$\begin{aligned} C_0&=1+a_1a_1^{*}+a_2a_2^{*}\\ &=2(1-\alpha-\beta+\alpha^2+\beta^2+\alpha\beta+\alpha\beta\cos\varphi),\\ C_1+C_1^{*}&=a_1+a_1^{*}+a_1a_2^{*}+a_1^{*}a_2\\ &=-2\varepsilon[\{\alpha-\beta+\beta(\alpha+\beta)\}\cos M\varphi\\ &\quad+\{\beta-\alpha+\alpha(\alpha+\beta)\}\cos(M+1)\varphi],\\ C_2+C_2^{*}&=a_2+a_2^{*}\\ &=-2(1-\alpha-\beta)\cos(2M+1)\varphi . \end{aligned}$$

Thus, we can calculate the denominator of equation (A3) as

$$\begin{aligned} C_0+C_1+C_1^{*}+C_2+C_2^{*}&=2[1-\alpha-\beta+\alpha^2+\beta^2+\alpha\beta\\ &\quad+\alpha\beta\cos\varphi-\varepsilon\{\alpha-\beta+\beta(\alpha+\beta)\}\cos M\varphi\\ &\quad-\varepsilon\{\beta-\alpha+\alpha(\alpha+\beta)\}\cos(M+1)\varphi\\ &\quad-(1-\alpha-\beta)\cos(2M+1)\varphi]. \end{aligned} \tag{A11}$$

The numerator of equation (A3) is calculated as follows:

$$\begin{aligned} D_0+D_1+D_1^{*}&=b_0(1+a_1+a_1^{*}+a_1a_1^{*}-a_2a_2^{*})\\ &\quad+b_1(1+a_1^{*}+a_2^{*})+\text{conj.}\\ &=\frac{2(1-\alpha)(1-\beta)(\alpha+\beta)}{2-\alpha-\beta}\Big[G_1^2+G_2^2\\ &\quad-2G_1G_2\cos\frac{\varphi}{2}-\varepsilon\Big\{G_1^2\cos(M+1)\varphi\\ &\quad+G_2^2\cos M\varphi-2G_1G_2\cos(2M+1)\frac{\varphi}{2}\Big\}\Big]\\ &=(1-\varepsilon)\frac{2(1-\alpha)(1-\beta)(\alpha+\beta)}{2-\alpha-\beta}\\ &\quad\times\left(G_1^2+G_2^2-2G_1G_2\cos\frac{\varphi}{2}\right)\\ &=(1-\varepsilon)\frac{2(1-\alpha)(1-\beta)(\alpha+\beta)}{2-\alpha-\beta} \end{aligned} \tag{A12}$$

because

$$G_1^2\cos(M+1)\varphi+G_2^2\cos M\varphi$$
$$-2G_1G_2\cos(2M+1)\frac{\varphi}{2}$$
$$=G_1^2+G_2^2-2G_1G_2\cos\frac{\varphi}{2}=1\,. \quad \text{(A13)}$$

Thus, we have finally

$$D(\varphi)=\frac{(1-\varepsilon)\dfrac{(1-\alpha)(1-\beta)(\alpha+\beta)}{2-\alpha-\beta}}{\begin{pmatrix}1-\alpha-\beta+\alpha^2+\beta^2+\alpha\beta+\alpha\beta\cos\varphi-\varepsilon\{\alpha-\beta+\beta(\alpha+\beta)\}\cos M\varphi\\ -\varepsilon\{\beta-\alpha+\alpha(\alpha+\beta)\}\cos(M+1)\varphi-(1-\alpha-\beta)\cos(2M+1)\varphi\end{pmatrix}}\,. \quad \text{(A14)}$$

From this equation, we have

$$\begin{cases} D(\varphi)=0 & \text{for } h+k\text{:even } i.e.\ \varepsilon=1\\ D(\varphi)=0 & \text{for } h+k\text{:odd } i.e.\ \varepsilon=-1\\ & \text{and } \alpha=1,\ \beta=1,\text{ or } \alpha=\beta=0 \end{cases} \quad \text{(A15)}$$

and, in other cases, equation (19).

APPENDIX II
Direct derivation of intensities for four special cases (§2) using (17) and (18)

In part I of this series, equations (8) and (10) were derived from the corresponding structures, *i.e.* $(M\mid\bar{M})$ and $(M\ \bar{M}+1)$ respectively. But the same results can be derived directly from equation (17) with equation (18) *i.e.*

$$I(\varphi)=Nb_0+\sum_{m=1}^{N-1}(N-m)b_m+\text{conj.} \quad \text{(A16)}$$

with

$$b_m=(\varepsilon\phi)^m\ \text{spur}\ \mathbf{vwq}^m$$
$$=\exp\{-im(M\varphi-\pi)\}\ \text{spur}\ \mathbf{vwq}^m. \quad \text{(A17)}$$

The unitary intensities of the superlattice reflexions for the four special cases shown in Fig. 3 (§2) are directly derived as follows:

Case (1) $\alpha=1$ *and* $0\le\beta<1$,*i.e.* $(M\mid\bar{M})$.

In this case, we have $w_1=1$ and $w_2=0$ from equation (3) and the necessary quantities become as follows:

$$\mathbf{w}=\begin{bmatrix}1&0\\0&0\end{bmatrix},\quad \mathbf{p}=\begin{bmatrix}1&0\\1-\beta&\beta\end{bmatrix}.$$

Therefore

$$\mathbf{vw}=\begin{bmatrix}v_1^*v_1&0\\v_2^*v_1&0\end{bmatrix},\quad \mathbf{q}=\begin{bmatrix}1&0\\(1-\beta)e^{-i\varphi}&\beta e^{-i\varphi}\end{bmatrix},$$

therefore

$$\mathbf{vwq}^m=\mathbf{vw}\,.$$

As a result, we get

$$b_m=v_1^*v_1\exp\{-im(M\varphi-\pi)\} \quad \text{(A18)}$$

and finally $I(\varphi)$ becomes

$$I(\varphi)=v_1^*v_1\frac{\sin^2 N_0(M\varphi-\pi)}{\sin^2\dfrac{M\varphi-\pi}{2}} \quad \text{(A19)}$$

where we put $N=2N_0$ because we have $P=2M$. From equation (A19), we have the Laue peaks only at

$$\frac{M\varphi-\pi}{2}=l'\pi\quad l'\text{: } 0,\ \pm1,\ \pm2,\ \ldots$$
$$i.e.\ \zeta=\frac{l}{P}\ \text{with } l\text{: odd}, \quad \text{(A20)}$$

and hence we get the result

$$\frac{I\begin{pmatrix}l\\P\end{pmatrix}}{N_0^2}=4(v_1^*v_1)_{\zeta=l/P}=\frac{4}{\sin^2\dfrac{\pi l}{P}}\ \text{with } l\text{: odd} \quad \text{(A21)}$$

in agreement with equation (8).

Case (2) $\beta=1$ *and* $0\le\alpha<1$, *i.e.* $(M+1\mid\bar{M}+1)$

In this case, we have $w_1=0$ and $w_2=1$ from equation (3) and the necessary quantities become as follows:

$$\mathbf{w}=\begin{bmatrix}0&0\\0&1\end{bmatrix},\quad \mathbf{p}=\begin{bmatrix}\alpha&1-\alpha\\0&1\end{bmatrix},$$

therefore

$$\mathbf{vw}=\begin{bmatrix}0&v_1^*v_2\\0&v_2^*v_2\end{bmatrix},\quad \mathbf{q}=\begin{bmatrix}\alpha&1-\alpha\\0&e^{-i\varphi}\end{bmatrix},$$

therefore

$$\mathbf{vwq}^m=\mathbf{vw}e^{-im\varphi}.$$

As a result, we get

$$b_m=v_2^*v_2\exp[-im\{(M+1)\varphi-\pi\}]\,. \quad \text{(A22)}$$

In a similar way to case (1), we can derive, by the use of equation (A22), the same result as equation (A21) with $P=2(M+1)$ and v_1 replaced by v_2.

Case (3) $\alpha=\beta=1$, *i.e.* $(M\mid\bar{M})$ *and* $(M+1\mid\bar{M}+1)$

In this case, from equation (7) we have only the relation $w_1+w_2=1$, and the necessary quantities become as follows:

$$\mathbf{w}=\begin{bmatrix}w_1&0\\0&w_2\end{bmatrix}\ \text{with } w_2=1-w_1,\quad \mathbf{p}=\begin{bmatrix}1&0\\0&1\end{bmatrix},$$

therefore

$$\mathbf{vw}=\begin{bmatrix}w_1v_1^*v_1&w_2v_1^*v_2\\w_1v_2^*v_1&w_2v_2^*v_2\end{bmatrix},\quad \mathbf{q}=\begin{bmatrix}1&0\\0&e^{-i\varphi}\end{bmatrix}=\boldsymbol{\phi},$$

therefore

$$\mathbf{vwq}^m = \mathbf{vw}\phi^m = \mathbf{vw}\begin{bmatrix}1 & 0\\ 0 & e^{-im\varphi}\end{bmatrix}.$$

Thus, we get

$$b_m = w_1 v_1^* v_1 \exp\{-im(M\varphi-\pi)\} + w_2 v_2^* v_2 \exp[-im\{(M+1)\varphi-\pi\}] \quad \text{(A23)}$$

and finally $I(\varphi)$ becomes

$$I(\varphi) = w_1 v_1^* v_1 \frac{\sin^2 N_0(M\varphi-\pi)}{\sin^2 \dfrac{M\varphi-\pi}{2}} + w_2 v_2^* v_2 \frac{\sin^2 N_0\{(M+1)\varphi-\pi\}}{\sin^2 \dfrac{(M+1)\varphi-\pi}{2}} \quad \text{(A24)}$$

which is the mean intensity of those due to $(M \mid \bar{M})$ and $(M+1 \mid \overline{M+1})$ with weights w_1 and w_2 respectively.

Case (4) $\alpha=\beta=0$, *i.e.* $(M\ \overline{M+1})$ *or* $(M+1\ \bar{M})$

In this case, we have $w_1=w_2=\frac{1}{2}$ from equation (3) and the necessary quantities become as follows:

$$\mathbf{w} = \tfrac{1}{2}\begin{bmatrix}1 & 0\\ 0 & 1\end{bmatrix}, \quad \mathbf{p} = \begin{bmatrix}0 & 1\\ 1 & 0\end{bmatrix}$$

therefore

$$\mathbf{vw} = \tfrac{1}{2}\mathbf{v}, \quad \mathbf{q} = \begin{bmatrix}0 & 1\\ e^{-i\varphi} & 0\end{bmatrix}, \quad \mathbf{q}^2 = e^{-i\varphi}\mathbf{I}$$

therefore

$$\mathbf{vwq}^m = \tfrac{1}{2}e^{-in\varphi} \times \begin{cases}\mathbf{v} & \text{for } m=2n\\ \mathbf{vq} & \text{for } m=2n+1.\end{cases}$$

As a result, we get

$$b_m = e^{-im\theta} \times \begin{cases}b_0 & \text{for } m=2n\\ G_1G_2 & \text{for } m=2n+1\end{cases} \quad \text{(A25)}$$

where

$$\begin{cases} b_0 = \frac{1}{2}(G_1^2+G_2^2)\\ \theta = (2M+1)\dfrac{\varphi}{2} - \pi = \dfrac{P\varphi}{2} - \pi, \quad P=2M+1 \end{cases} \quad \text{(A26)}$$

and G_1 and G_2 are given by equation (A9). Finally with $N=2N_0$, $I(\varphi)$ becomes,

$$I(\varphi) = 2b_0\left\{N_0 + \sum_{n=1}^{N_0-1}(N_0-n)e^{-in2\theta} + \text{conj.}\right\} + G_1G_2\left[N + \sum_{m=1}^{N-1}(N-m)e^{-im\theta} + \text{conj.} - 2\left\{N_0 + \sum_{n=1}^{N_0-1}(N_0-n)e^{-in2\theta} + \text{conj.}\right\}\right]$$
$$= (G_1^2+G_2^2+2G_1G_2\cos\theta)\frac{\sin^2 N_0\theta}{\sin^2\theta}. \quad \text{(A27)}$$

Equation (A27) gives the Laue peaks at

$$\zeta = \frac{l}{P} \quad l: 0, \pm1, \pm2, \ldots$$

at which we have

$$\frac{I\left(\begin{matrix}l\\P\end{matrix}\right)}{N_0^2} = \{G_1^2+G_2^2-(-1)^l 2G_1G_2\}_{\zeta=l/p} = \begin{cases}\dfrac{1}{\cos^2\dfrac{\pi l}{2P}} & \text{for } l\text{: even}\\[2ex] \dfrac{1}{\sin^2\dfrac{\pi l}{2P}} & \text{for } l\text{: odd}\end{cases} \quad \text{(A28)}$$

in agreement with equation (10).

The author would like to express his sincere thanks to Professor J. Kakinoki for his kind guidance and for many helpful discussions.

References

FUJIWARA, K. (1957). *J. Phys. Soc. Japan*, **12**, 7.

FUJIWARA, K., HIRABAYASHI, M., WATANABE, D. & OGAWA, S. (1958). *J. Phys. Soc. Japan*, **13**, 167.

HIRABAYASHI, M. & OGAWA, S. (1957). *J. Phys. Soc. Japan*, **12**, 259.

JEHANNO, G. & PÉRIO, P. (1962). *J. Phys. Radium*, **23**, 854.

KAKINOKI, J. (1971). Private communication.

KAKINOKI, J. & KOMURA, Y. (1965). *Acta Cryst.* **19**, 137.

KAKINOKI, J. & MINAGAWA, T. (1971). *Acta Cryst.* A**27**, 647.

KAKINOKI, J. & MINAGAWA, T. (1972). *Acta Cryst.* A**28**, 120.

SCHUBERT, K., KIEFER, B., WILKENS, M. & HAUFLER, R. (1955). *Z. Metallk.* **46**, 692.

SCOTT, R. E. (1960). *J. Appl. Phys.* **31**, 2112.

TOTH, R. S. & SATO, H. (1962). *J. Appl. Phys.* **33**, 3250.

WATANABE, D. & OGAWA, S. (1956). *J. Phys. Soc. Japan*, **11**, 226.

YAKEL, H. L. (1962). *J. Appl. Phys.* **33**, 2439.

YAMADA, Y., SHIBUYA, I. & HOSHINO, S. (1963). *J. Phys. Soc. Japan*, **18**, 1594.

YAMAGUCHI, S., WATANABE, D. & OGAWA, S. (1962). *J. Phys. Soc. Japan*, **17**, 1902.